Publisher's PDF, also known as Version of record

Link to published version (if available):
10.1103/PhysRevLett.94.073903

Link to publication record in Explore Bristol Research
PDF-document

Real-Space Observation of Ultraslow Light in Photonic Crystal Waveguides

H. Gersen,[1,*] T. J. Karle,[2] R. J. P. Engelen,[1] W. Bogaerts,[3] J. P. Korterik,[1] N. F. van Hulst,[1] T. F. Krauss,[2] and L. Kuipers[1,4,†]

[1]*Applied Optics Group, Department of Science Technology and MESA$^+$ Institute for Nanotechnology, University of Twente, P.O. Box 217, 7500 AE Enschede, The Netherlands*
[2]*Ultrafast Photonics Collaboration, School of Physics and Astronomy, University of St. Andrews, St. Andrews, Fife, KY16 9SS, United Kingdom*
[3]*Ghent University–IMEC, Department of Information Technology (INTEC), B-9000 Gent, Belgium*
[4]*FOM-Institute for Atomic and Molecular Physics (AMOLF), Kruislaan 407, 1098 SJ Amsterdam, The Netherlands*
(Received 3 September 2004; published 25 February 2005)

We show the real-space observation of fast and slow pulses propagating inside a photonic crystal waveguide by time-resolved near-field scanning optical microscopy. Local phase and group velocities of modes are measured. For a specific optical frequency we observe a localized pattern associated with a flat band in the dispersion diagram. During at least 3 ps, movement of this field is hardly discernible: its group velocity would be at most $c/1000$. The huge trapping times without the use of a cavity reveal new perspectives for dispersion and time control within photonic crystals.

Scientists have long been trying to capture and manipulate light with an all-optical analogue to the electronic silicon chip. Photonic band gap materials, periodic dielectric structures that mimic the properties of semiconductors to guide and trap light [1], have already enabled the creation of micrometer sized lasers [2], waveguides [3], and nanocavities [4] by confining the light on a wavelength scale. Fast signals in optical structures have a broad spectrum and therefore sample the (material) dispersion over a wide range. Photonic crystal (PhC) structures that allow the control and compensation of dispersion therefore become increasingly important [5,6]. PhCs exhibiting dispersion control enable the selective retardation of optical signals via ultraslow light propagation, e.g., for optical delay lines [7], enhanced light-matter interaction [5], or quantum information processing [8].

Experimental verification of dispersive phenomena in PhCs, however, is still a difficult and demanding issue [9]. Only indirect measurements of the group velocity and its dispersion have been reported so far [5,10–12]. In general, these methods rely either on using a reference structure or on so-called "cutback methods." As signals are collected outside the structure of interest, little direct insight into the behavior and the evolution of pulses inside the structure is obtained. To take a direct look inside a PhC is, however, far from trivial as conventional microscopy is limited by the diffraction limit. Furthermore, guided PhC waveguide (PhCW) modes are evanescent in air and can therefore not be observed with far-field techniques. Circumventing these restrictions is possible by bringing a subwavelength-sized probe into the evanescent fields close to a sample surface. The few near-field scanning optical microscopy (NSOM) experiments on PhCs so far detected only field intensities [13–15]. However, letting the collected light interfere with a frequency shifted reference beam gives access to the local field amplitude and phase [16]. The combination with the use of ultrashort pulses (see Fig. 1) allows the direct visualization of dynamic effects inside the structure [17,18].

Here, we use this technique to visualize fast and slow pulses as they propagate inside a PhCW. For a specific optical frequency, a complex, localized stationary modal pattern is observed associated with a flat band in the measured dispersion diagram. This pattern persists for more than 3.6 ps after the excitation pulse has moved away. This constitutes a "trapping time" of the same order of magnitude as that of state-of-the-art photonic crystal cavities [4]. However, this pattern is not associated with any cavity or the like. Nevertheless, we observe that it
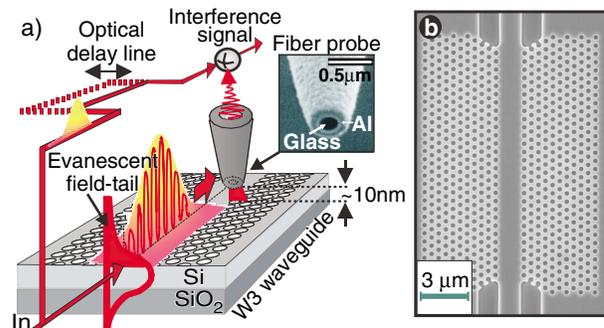

FIG. 1 (color). (a) Schematic representation of a pulse tracking experiment on a W3 PhCW. The evanescent field of a propagating pulse is picked up by a metal coated fiber probe with a subwavelength-sized aperture and interferometrically mixed with light from a reference branch. The inset shows the probe used in the experiment. The aperture size ($\phi = 240$ nm) in the first approximation determines the optical resolution. Measurements are done by raster scanning the optical probe across the structure at a constant height (<10 nm). (b) Top view of the PhCW under study, although with a shorter device length.

moves by less than 0.9 μm in 3 ps, suggesting an upper limit for the group velocity of less than $c/1000$.

The PhCWs were fabricated on a silicon-on-insulator wafer, with a 220 nm thick silicon (Si) waveguide layer on top of a 1 μm thick silicon dioxide (SiO_2) cladding [19]. Holes are arranged in a hexagonal array [period $a = 400$ and 460 nm, hole radius $r = 130$ nm, and three rows of missing holes define the so-called W3 PhCW; see Fig. 1(b)]. Linearly TE-polarized light ($E \parallel$ to crystal plane) is coupled to the PhCW.

Figure 2 shows how ultrafast pulses can be tracked through a W3 PhCW with a local time-resolved heterodyne interference measurement. Short transform-limited Gaussian pulses (FWHM 120 ± 10 fs, $\Delta\omega \approx 0.02$) were launched in the access waveguide at a wavelength (λ) of 1245 ± 0.5 nm ($\omega = 0.3695$). In the measured topography of the PhCW [Fig. 2(a)] the entrance and exit waveguides are clearly resolved. One can also recognize the pattern of holes ($a = 460$ nm) that forms the PhC. The measured optical amplitudes for increasing reference times are shown [Figs. 2(b)–2(g)]. We observe the separation of the incoming pulse in multiple pulses with different modal distributions. It is immediately clear that the different modes propagate with largely different group velocities [20].

The time evolution of individual modes can be extracted from these local measurements [21]. For each pulse mea-
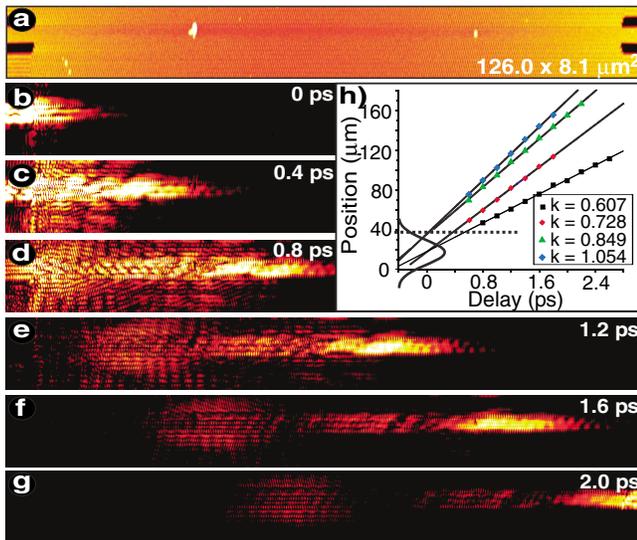

FIG. 2 (color).   A time-resolved NSOM measurement on a W3 PhCW ($a = 460$ nm). (a) Topographic image of the structure rotated 90° with respect to Fig. 1(b). (b)–(g) The optical amplitude in the W3 PhCW for different reference times (400 ± 1 fs between frames; all frames have the same color scale). A movie displaying the pulse propagation is available [20]. It is apparent that pulses with different modal distributions and group velocities are excited in the W3 waveguide. (h) The measured position of the center of mass for pulses with different modal distributions (and different wave vectors) as a function of the delay time. The dotted line represents the start of the PhC.

surement the raw data correspond to the amplitude times the cosine of the phase [18]. A spatial Fourier transform (SFT) directly reveals the spatial frequencies present in the raw data. The various modes excited in the waveguide show up as individual peaks in the SFT. Applying an inverse Fourier transform to a selected peak allows the spatial position of the pulse in that mode to be determined. Repeating this procedure for successive frames yields the pulse position as a function of time. When the observed pulses are roughly Gaussian and retain their shape during propagation, the change in the position of the " center of mass" (c.m.) is an unambiguous measure for the group velocity [18]. Figure 2(h) shows the position of the c.m. as a function of the reference time for several modes. A linear fit yields the group velocity of these modes. We observe a group velocity as small as $(0.121 \pm 0.001) \times c$, with c the vacuum speed of light. The highest measured group velocity is $(0.243 \pm 0.001) \times c$. However, not all of the experimentally observed modes in the PhCW have been depicted in Fig. 2(h). For those modes ($k = 0.797, 0.936,$ and 0.984) the pulse shape was found to change strongly as a function of time. This is the result of a very strong group-velocity dispersion (GVD). Using an analytical model [18] we calculate that for the strongest dispersed mode at $k = 0.797$ the GVD is at least as large as 3×10^5 ps^2/km. The observed GVD for this specific mode is almost 5 orders of magnitude larger than in a conventional single-mode optical fiber (typically 8 ps^2/km at 1245 nm).

Note that extrapolation of the fitted lines [Fig. 2(h)] indicates that the various modes are not excited at the same time at the start of the crystal. The observed time delay between excitation of the different modes in Fig. 2(h) can be as large as 500 fs. The time lags are caused by multiple modes in the entrance waveguide. In a conventional "time-of-flight" measurement, in which the sample is treated as a "black box," such an (in principle undesired) excitation by higher order modes could, for short device lengths, lead to the erroneous conclusion that very small group velocities are observed.

The phase sensitivity of the technique can be exploited to determine the local photonic band structure experimentally. For a certain ω a SFT of the raw data reveals the spatial frequencies and hence propagation constants. Varying ω therefore yields the band structure. Figure 3(a) displays the SFT of the data for all wavelengths accessible in our experiment (1180–1350 nm, wavelength step 5 nm) on two different PhCWs ($a = 400$ and 460 nm, respectively). The vertical axis displays the excitation wavelength in terms of ω, while the horizontal axis corresponds to the observed spatial frequencies. For a wide defect waveguide such as the W3, the principle components of the field follow roughly the same dispersion as a nonperiodic waveguide of identical proportions. The six positive slopes visible in Fig. 3(a) for $0.5 < k < 1$ agree well with the first six TE-polarized modes calculated for such a nonperiodic waveguide [22].
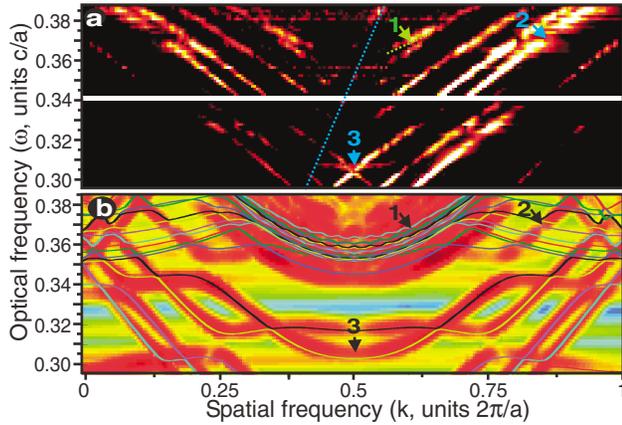
FIG. 3 (color). (a) Experimental dispersion diagram of the
modes excited in the W3 PhCW. Displayed is the spatial
Fourier transform of data for multiple excitation frequencies.
The location of the slowest mode ($k = 0.607$) observed in Fig. 2
is indicated by 1. Its measured group velocity gives an indepen-
dent measure for the slope of its dispersion curve (green dotted
line). (b) Simulated dispersion diagram. The local slope of the
calculated band structure for $k = 0.607$ (indicated by 1) gives an
expected group velocity of $0.115 \times c$ in good agreement with the
measured value of $(0.121 \pm 0.001) \times c$. Comparing Fig. 3(b)
with the measured band structure in Fig. 3(a) reveals a flat band
around $\omega = 0.305$ (indicated by 3).

The effect of the periodic modulation of the refractive
index on the propagating modes can be calculated by
directly solving time-dependent Maxwell equations with
a 2D finite-difference time domain (FDTD) method.
Fourier transformation of the calculated fields for multiple
excitation frequencies yields the expected band structure
shown in Fig. 3(b) [23]. The overlaid solid lines depict the
band structure calculated by a plane wave method. First,
the periodicity introduces additional wave vector com-
ponents, which are visible in Fig. 3(a) for $0 < k < 0.5$.
Second, the folding of modes causes modes to cross, cre-
ating gaps in the lines due to the avoided crossings, for
which an indication is, e.g., observed in the region indi-
cated by 2. Good agreement is found between the mea-
sured group velocities and the slopes ($d\omega/dk$) in the ex-
perimental and calculated band diagrams. However, com-
parison of the region indicated by 3 in Fig. 3 shows that
there are clear differences between experiment and theory.
Preliminary calculations for a nonperiodic waveguide in-
dicate that the positive slope visible in Fig. 3(a) at this
region [and not in Fig. 3(b)] agrees with a fourth order TE
mode [22].

Close inspection of the region indicated by 3 in Fig. 3(a)
shows the presence of a flat PhCW mode at the Brillouin
zone boundary. This flat band is also clearly visible in the
simulated band structure depicted in Fig. 3(b). Figure 4
presents pulse tracking measurements for this flat band
($\omega = 0.305$), with 4(a) the measured topography. In
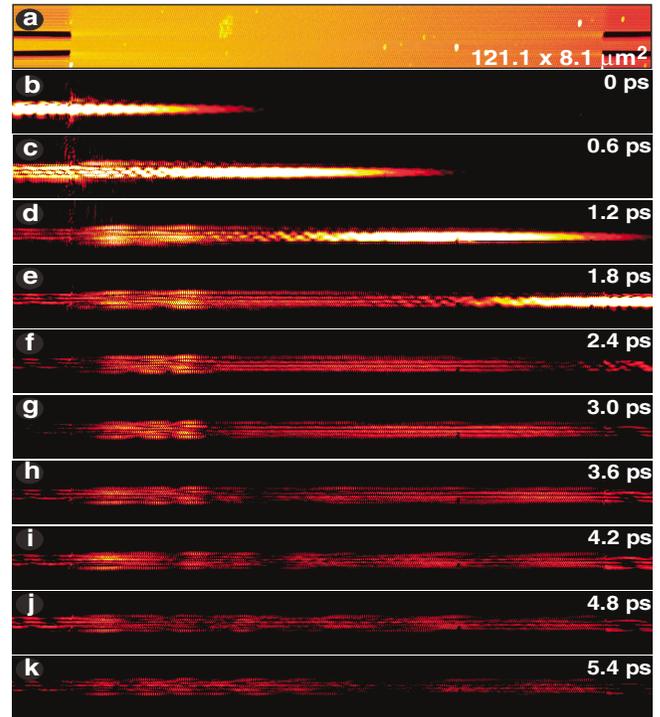Figs. 4(b)–4(k) the optical amplitude is depicted as a

FIG. 4 (color). Pulse tracking experiment at a flat band at $\omega =
0.305$ ($\lambda = 1310$ nm, $a = 400$ nm). (a) Topography of the
PhCW. (b)–(k) The optical amplitude as a function of reference
time (all frames have the same color scale). A movie displaying
the pulse propagation is available [20]. We observe a complex
and stationary localized modal pattern in the first 25 μm of the
PhCW which exists for more than 3.6 ps after the excitation
pulse has moved away. The field pattern moves by less than
0.9 μm in 3 ps, suggesting a group velocity of less than $c/1000$.
Note that all light observed in (f) through (k) belongs to the same
mode located between $k = 0.4$–0.6, unlike in Fig. 2 where
various discrete wave vectors are present simultaneously.

function of the reference time in steps of 600 ± 1 fs.
Several dynamic phenomena are apparent. First, we ob-
serve a first order mode pulse propagating through the
structure in Figs. 4(b)–4(e). Second, in the wake of this
pulse, striking effects are visible. Fascinatingly, a localized
and stationary optical field is observed which persists for
very long times. It is located in the first 25 μm behind the
entrance of the PhCW. The pattern is reminiscent of the
patterns associated with mini-stopgaps [24,25]. Despite the
fact that the PhCW is an open structure and no resonant
cavity is present, the optical field persists for more than
3.6 ps. This trapping time can be compared to the quality
factor Q of a resonator via $Q = \omega\tau$, where ω is the optical
frequency and τ the trapping time of light. The trapping
time of 3.6 ps is equivalent to a Q of 6×10^3. After
roughly 3.6 ps the spatial shape of the field alters, but
even after 5 ps light with a comparable symmetry is still
present in the structure. Between 1.2 and 4.2 ps, movement
of this localized light field is hardly discernible: if a group
velocity should be assigned, it would be at most $c/1000$.

Note that the localized field is not excited directly at the start of the PhCW. A pulse excited directly at the start, propagating at $c/1000$, would have taken many nanoseconds before arriving at the location where we observe it. This is clearly not the case, indicating that this is not just a simple slow pulse propagating near a photonic band edge.

Our observation clearly demonstrates that a guided mode with an extremely slow velocity and very large group-velocity dispersion is excited in the PhCW. It is often thought that it is hard to excite such a slow mode due to the large mismatch in group velocities. Apparently, the special situation of an index guided mode with the proper modal symmetry interacting with a slow mode at the Brillouin boundary allows efficient excitation of the ultraslow light field. Although not easy, specific modes for excitation can be generated by careful design of mode converters and couplers and could lead to very efficient coupling to slow modes [26]. The huge trapping times observed without the use of a cavity should therefore open perspectives for new schemes of dispersion and time control of optical signals within photonic crystals.

———————————

*Current address: Interdisciplinary Nanoscience Center (iNANO), Center for Atomic-scale Materials Physics (CAMP) and Department of Physics and Astronomy, University of Aarhus, DK 8000 Aarhus C, Denmark.
†Corresponding author.
Electronic address: l.kuipers@amolf.nl

[1] J. D. Joannopoulos, R. D. Meade, and J. N. Winn, *Photonic Crystals: Molding the Flow of Light* (Princeton University Press, Princeton, NJ, 1995).
[2] O. Painter *et al.*, Science **284**, 1819 (1999).
[3] T. F. Krauss, R. M. De La Rue, and S. Brand, Nature (London) **383**, 699 (1996).
[4] Y. Akahane *et al.*, Nature (London) **425**, 944 (2003).
[5] M. Notomi *et al.*, Phys. Rev. Lett. **87**, 253902 (2001).
[6] T. J. Karle *et al.*, J. Lightwave Technol. **22**, 514 (2004).
[7] M. F. Yanik and S. Fan, Phys. Rev. Lett. **92**, 083901 (2004).
[8] M. D. Lukin and A. Imamoglu, Nature (London) **413**, 273 (2001).
[9] X. Letartre *et al.*, Appl. Phys. Lett. **79**, 2312 (2001).
[10] A. Imhof *et al.*, Phys. Rev. Lett. **83**, 2942 (1999).
[11] Yu. A. Vlasov *et al.*, Phys. Rev. E **60**, 1030 (1999).
[12] K. Inoue *et al.*, Phys. Rev. B **65**, 121308(R) (2002).
[13] P. L. Phillips *et al.*, J. Appl. Phys. **85**, 6337 (1999).
[14] S. I. Bozhevolnyi *et al.*, Phys. Rev. B **66**, 235204 (2002).
[15] P. Kramper *et al.*, Phys. Rev. Lett. **92**, 113903 (2004).
[16] E. Flück *et al.*, J. Lightwave Technol. **21**, 1384 (2003).
[17] M. L. M. Balistreri *et al.*, Science **294**, 1080 (2001).
[18] H. Gersen *et al.*, Phys. Rev. E **68**, 026604 (2003).
[19] W. Bogaerts *et al.*, Opt. Express **12**, 1583 (2004).
[20] See EPAPS Document No. E-PRLTAO-94-078510 for a high resolution version of Fig. 2 and movies of the pulse propagation through the PhCW. The available movies correspond to the data in Figs. 2 and 4, respectively. A direct link to this document may be found in the online article's HTML reference section. The document may also be reached via the EPAPS homepage (http://www.aip.org/pubservs/epaps.html) or from ftp.aip.org in the directory/epaps/. See the EPAPS homepage for more information.
[21] H. Gersen *et al.* Phys. Rev. E **70**, 066609 (2004).
[22] Calculated by a 1D mode solver (CAMFR); width $= 2\sqrt{3}a - 2r = 1.29 \,\mu m$, $a = 460$ nm, $n_{\text{eff}} = 2.89$.
[23] A preliminary 3D FDTD simulation including the SiO$_2$ cladding layer yields similar results.
[24] S. Olivier *et al.*, Phys. Rev. B **63**, 113311 (2001).
[25] M. Agio and C. M. Soukoulis, Phys. Rev. E **64**, 055603(R) (2001).
[26] J. Witzens and A. Scherer, J. Opt. Soc. Am. A **20**, 935 (2003).